Available online at www.sciencedirect.com
ScienceDirect
International Journal of Multiphase Flow 33 (2007) 1006–1022
International Journal of Multiphase Flow
www.elsevier.com/locate/ijmulflow

Kinetic modeling of particles in stratified flow – Evaluation of dispersion tensors in inhomogeneous turbulence

Roar Skartlien *

Institute for Energy Technology, P.O. Box 40, N-2027 Kjeller, Norway

Received 1 November 2006; received in revised form 14 April 2007

Abstract

The continuum equations for a dilute particle distribution in inhomogeneous turbulence are tested against results from a Langevin particle tracking simulation. Reeks' version of the kinetic theory is used to generate the mass, momentum and kinetic stress equations for the particle distribution. The particle tracking data are used to directly evaluate the dispersion tensors λ and μ which serve as closure relations for the continuum equations. These exact forms are compared to approximate, local forms. Even for low Stokes numbers (corresponding to low particle inertia defined by $\tau/\tau_p \gg 1$), the tensor λ is strongly affected by the inhomogeneity and depends on turbulence parameters in the volume corresponding to the particle path dispersion over the particle Lagrangian integral timescale τ. In contrast, the locally homogeneous form of the velocity dispersion tensor μ is a sufficient approximation, since it depends on the dispersion volume over the much smaller particle relaxation time τ_p. It is demonstrated that the body force due to the dispersion vector γ cannot be neglected. In the limit of passive tracers (zero stopping distance), γ is equal to the gradient of λ, if the physical setting is such that we can invoke constant tracer density in this limit.

Keywords: Suspensions; Particle diffusivity; Turbophoresis; Particle continuum equations; Kinetic theory; Langevin turbulence model

1. Introduction

In flows of particulate suspensions, sufficiently general physical models for the fluid–particle mixture are essential. For example, deposition rates near boundary layers and particle transport within the bulk of the carrier fluid may depend strongly on turbulence inhomogeneity, and one would therefore prefer a model which can handle the associated effects on the particle concentration and the particle kinetic stress. Kinetic theories for dilute suspensions (e.g., Reeks, 1992, 2005; Swailes and Darbyshire, 1999; Hyland et al., 1999; Sergeev et al., 2002; Zaichik and Alipchenkov, 2005) are sufficiently general such that turbulence inhomogeneity is accounted for in a consistent manner. A common factor in these theories is that they are formulated in terms of a conservation equation for the particle probability distribution function (PDF). The PDF itself is a function of time,

* Tel.: +47 63 80 64 67; fax: +47 63 81 11 68.
E-mail address: roar.skartlien@ife.no

0301-9322/$ - see front matter © 2007 Elsevier Ltd. All rights reserved.
doi:10.1016/j.ijmultiphaseflow.2007.04.001

space and particle velocity. The governing equation is the Liouville equation – a generalization of the Fokker–Planck equation for Brownian motion, to handle a non-zero correlation time of the turbulent driving force. The Liouville equation also shares similarities with the classical Boltzmann equation, with the replacement of the Boltzmann collision term with the particle-turbulence momentum transfer term (for a dilute flow). The kinetic approach can also handle a variety of wall boundary conditions, such as reflecting or partially reflecting walls, which the traditional two-fluid approach cannot do (e.g., Swailes and Reeks, 1994).

We will in the following work with the set of continuum equations which govern the velocity moments of the PDF (mass, momentum and kinetic stress). Physical models for solid particles, droplets and bubbles in turbulent pipe flow, are examples where kinetic theory may be considered as a foundation. A great advantage is the *non-phenomenological* character of the continuum equations, with consistency from the particle equation of motion to quantities such as concentration profiles. The two basic assumptions in the theory are: (a) The turbulent velocity fluctuations in the carrier phase as seen by the particles obey Gaussian statistics (for the purpose of obtaining exact dispersion tensor closure relations) and (b) The particle equation of motion adopts a driving force which is linear in the velocity difference between the particle and the carrier fluid (transversal lift forces may be included in the same framework). The corresponding drag coefficient β is assumed to be a constant. For non-linear drag one can perform a linearization procedure such that β becomes a function of the relative mean velocity between the particles and the fluid (e.g., Reeks, 1992). We also note that the background turbulence is considered as input to the model. When the suspension is dense such that back reaction on the turbulence is important, one has to model this effect in addition.

The central point of the current paper is to evaluate the dispersion tensors, with particular focus on the kinetic theory of Reeks (1992). These dispersion tensors are in effect closure relations entering in the continuum equations. The dispersion tensors can be expressed in terms of fluid velocity correlation functions as measured along the paths of the massive particles. There have been very few or no published attempts to derive explicit forms of the dispersion tensors in inhomogeneous turbulence (except to a certain degree in Devenish et al., 1999) which are more general than adopting the *locally homogeneous approximation* (LHA). It is therefore both interesting and desirable to find dispersion tensor approximations which are more applicable to inhomogeneous turbulence such that kinetic theory (KT) can be applied to a wider range of problems.

We will evaluate the kinetic theory by using data from a particle tracking simulation (PT) which follows individual particles via the equation of motion. The essential feature of the PT-approach is that the turbulent fluid velocity seen by the particle is modeled by a stochastic Langevin differential equation with a white noise source and a memory characterized by a local correlation timescale τ (Thomson, 1984; Iliopoulos and Hanratty, 1999 or Mito and Hanratty, 2005). The Langevin equation will be valid as long as we can generate the correct statistics of the turbulent driving force (or fluid velocity) following the particle. Thomson (1984) has shown that a drift term must be included in the Langevin equation to counteract the associated "spurious drift" which occurs in inhomogeneous turbulence. The PT data will be treated as the reference data set which are to be modeled by the mass, momentum and kinetic stress equations, and we will test the applicability of the LHA dispersion tensors, and the PT-evaluated "exact" dispersion tensors.

Section 2 reviews the kinetic theory and the method of particle tracking. The dispersion tensors and the kinetic model are evaluated in Section 3 by comparison to PT-data. Section 4 discusses the mass flux balance from kinetic theory in relation to the work of Mito and Hanratty (2005). The discussion and conclusions are presented in Section 5.

2. Physical framework and models

This section gives a brief summary of the meaning of the kinetic theory, the continuum equations and the dispersion tensors. The solution of the equations is presented for the 1D steady state case. The Langevin particle tracking method is summarized and the specific physical setting for the numerical experiment to follow is specified.

2.1. The Liouville PDF equation for the particles

Reeks' (1992, 1993) continuum model for particles in a turbulent fluid will be adopted in the following. This theory is founded on a linear particle equation of motion,

$$\frac{\mathrm{D}\mathbf{v}}{\mathrm{D}t} = \mathbf{F}/m_\mathrm{p} = \underline{\beta}\cdot(\mathbf{u}-\mathbf{v}) + \left(1-\frac{\rho_\mathrm{c}}{\rho_\mathrm{p}}\right)\mathbf{g},$$

where $\mathbf{u}$ is the fluid velocity, $\mathbf{v}$ the particle velocity and $\underline{\beta}$ is a tensor accounting for lift and drag. The drag coefficients are represented by the diagonal components of the tensor. This linearized form is a first order approximation to the generally non-linear hydrodynamic forces exerted on the particle. The material densities of the carrier fluid and the particle are ρ_c and ρ_p, respectively. We will in the following assume dense particles in the sense $\rho_\mathrm{c}/\rho_\mathrm{p} \ll 1$, giving

$$\frac{\mathrm{D}\mathbf{v}}{\mathrm{D}t} = -\underline{\beta}\cdot\mathbf{v} + \langle\mathbf{f}\rangle + \mathbf{f}' + \mathbf{g}, \tag{1}$$

where the fluctuating force due to turbulence is $\mathbf{f}' = \underline{\beta}\cdot\mathbf{u}'$, and the average force is $\langle\mathbf{f}\rangle = \underline{\beta}\cdot\langle\mathbf{u}\rangle$. For a collisionless "particle gas", the ensemble averaged Liouville equation over all realizations of the gas turbulence ($\mathbf{f}'$) is

$$[\partial_t + \mathbf{v}\cdot\nabla_\mathbf{x} + \nabla_\mathbf{v}\cdot(-\underline{\beta}\cdot\mathbf{v} + \langle\mathbf{f}\rangle + \mathbf{g})]\langle W\rangle = -\nabla_\mathbf{v}\cdot\langle\mathbf{f}'W\rangle, \tag{2}$$

where the phase space "diffusion current" is

$$\mathbf{j} = \langle\mathbf{f}'W\rangle \tag{3}$$

and where $W = W(\mathbf{x},\mathbf{v},t)$ is the phase space distribution function corresponding to a single realization of $\mathbf{f}'$. The diffusion current serves to modify the distribution function according to the turbulent forcing on the particles.

The main advantage with working in phase space is that there exists an exact closure for the diffusion current in terms of $\langle W\rangle$, provided that Gaussian statistics can be assumed for $\mathbf{f}'$. The closure relation is, when written out in component form (Reeks, 1992; Hyland et al., 1999)

$$j_k = -(\partial_{v_j}\mu_{jk} + \partial_{x_j}\lambda_{jk} + \gamma_k)\langle W\rangle, \tag{4}$$

where the dispersion tensors are μ_{ij}, λ_{ij} and γ_j. The first two dispersion tensors account for the broadening or diffusion of the distribution function along the velocity and space axes, respectively. In particular, in the limit of passive tracer particles (limit of zero inertia), λ_{ij} is proportional to the passive scalar diffusivity characterizing the carrier fluid. The dispersion vector γ_j represents a drift speed along the velocity axis which corresponds to an additional particle acceleration due to inhomogeneity of the turbulence. In later versions of the theory (Reeks, 2001, 2005), the dispersion tensors are defined in a slightly different manner. The drift term due to γ_j is then expressed in terms of the divergence of the particle velocity field, which in the limit of passive tracer particles in an incompressible fluid vanishes automatically. We will enforce this limiting behavior in the 1992-version of the theory by properly constraining the drift term, as shown in the PSA-approximation below.

The dispersion tensors depend on the fluid turbulence in the following manner:

$$\mu_{jk} = \langle\Delta v_j(\mathbf{x},\mathbf{v},t)f_k'(\mathbf{x},t)\rangle,$$
$$\lambda_{jk} = \langle\Delta x_j(\mathbf{x},\mathbf{v},t)f_k'(\mathbf{x},t)\rangle,$$
$$\gamma_k = -\langle\Delta x_j(\mathbf{x},\mathbf{v},t)\partial_{x_j}f_k'(\mathbf{x},t)\rangle.$$

These relations are general, valid also in inhomogeneous turbulence. The quantities $\Delta\mathbf{x}$ and $\Delta\mathbf{v}$ are position and velocity changes due to $\mathbf{f}'$ along a particle trajectory. The relations between the force and the displacements are described by the appropriate Green's function (impulse response) of the particle equation of motion. This is described in more detail below for the 1D case. The particle trajectory intersects $(\mathbf{x},\mathbf{v})$ at time t in phase space (and starts at an earlier time t_1). The ensemble average (angle brackets) are taken over all such trajectories intersecting $(\mathbf{x},\mathbf{v})$ at time t. The initial conditions define a subset of all possible trajectories.

2.2. Continuum equations in 1D stratified flow

The continuum equations are derived, as usual, by taking velocity moments of the governing PDF equation. The first three moments of the Liouville equation generates the mass, momentum and kinetic stress

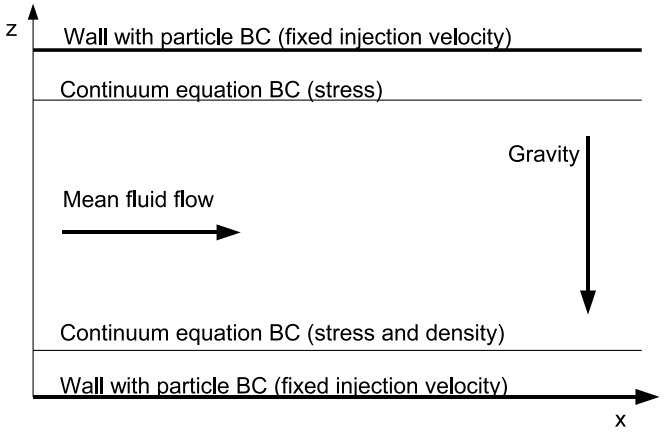

Fig. 1. *Channel geometry.* Gravity acts in the wall normal z-direction, and the mean fluid flow is parallel to the walls (in the x-direction). The flow is fully developed such that all physical quantities vary only in the z-direction, making the problem one-dimensional. The wall has a no-slip boundary condition for the fluid, such that the standard channel flow fluid turbulence statistics can be used. For the PT-simulation, the particles are absorbed and then re-injected with the friction velocity at the walls. The continuum equation boundary conditions for the particles are given at two interior locations, with stress and density values taken from the PT-simulation.

equations for the particles. The kinetic stress equation is supplied with a closure relation for the energy flux in order to limit the number of equations.[1]

In the current case, we will restrict ourselves to 1D geometry which is appropriate for a stratified, turbulent, steady state flow. Consider an infinite channel between two horizontal boundaries where the mean fluid velocity is parallel to the boundaries and possesses a shear. Gravity acts in the vertical direction (z) perpendicular to the boundaries. See Fig. 1. The fluid turbulence is assumed to be stationary (fully developed) and not affected by the presence of the particles. The turbulence intensities, stress, etc. can then be considered as given input parameters, varying only in the vertical direction. Lift forces are neglected such that a diagonal isotropic drag tensor $\beta_{ij} = \delta_{ij}\beta$ is imposed, where $\beta^{-1} = \tau_p$ is the particle relaxation time. The equations for vertical and horizontal momentum then become decoupled such that only the vertical component of the normal stress is needed. The corresponding 1D continuum equations read

$$\partial_t \rho + \partial_z(\rho \bar{v}_z) = 0, \tag{5}$$

$$\partial_t(\rho \bar{v}_z) + \partial_z(\rho \bar{v}_z^2 + T_{zz}) = -\rho(\beta \bar{v}_z + g + \bar{\gamma}_z), \tag{6}$$

$$\partial_t(\rho E_z) + \partial_z(\rho E_z \bar{v}_z) = -2\beta\rho E_z + \partial_z(\rho \epsilon_{zz} \partial_z E_z) - T_{zz}\partial_z \overline{v_z} + \rho \bar{\mu}_{zz}. \tag{7}$$

Overbars denote particle density weighted averages (the average of the particular quantity over all particle velocities at z) defined by the distribution $\langle W \rangle$. The mean particle velocity is $\bar{v}_z$ and the average particle density is ρ (skipping the overbar). In the literature regarding particles in turbulence, the density ρ of particles is often referred to as the concentration.

The (z,z) component of the particle stress tensor is

$$T_{zz} = \rho(2E_z + \bar{\lambda}_{zz}). \tag{8}$$

We note that the associated particle pressure is

$$P = 1/3(T_{xx} + T_{yy} + T_{zz}). \tag{9}$$

The contribution to the specific kinetic energy from normal stress is

$$E_z = (1/2)\overline{v_z' v_z'} \tag{10}$$

[1] A similar procedure can be used to derive the Navier–Stokes equations, but then with the Boltzmann equation as the governing phase space PDF equation.

and the (z,z) component of the diffusion tensor is generally

$$\epsilon_{zz} = T_{zz}/(\rho\beta). \tag{11}$$

In general, the dispersion coefficient ϵ_{ij} has two contributions, the dispersion induced by the mean shear in the flow, and the dispersion induced by turbulence (Section 2.4). It can be shown that the shear contribution is zero for the wall normal component ϵ_{zz} in *homogeneous* flows when the mean flow is parallel to the walls. We will assume that the shear contribution to ϵ_{zz} vanishes also in the case for inhomogeneous flows, such that ϵ_{zz} may be regarded as a (non-local) turbulent particle diffusivity in the following.

The continuity equation (5) is in the familiar form. The right hand side of the momentum equation (6) has a friction term linear in β, and a momentum source or net body force $-\rho\bar{\gamma}_z$ due to turbulence. This turbulent force is non-zero in inhomogeneous turbulence and must therefore be accounted for in most flow situations. Note that this body force is only contained in the momentum equation. One can recast the momentum equation as a generalized diffusion equation expressing the contributions to the mass flux $\rho\bar{v}_z$. The associated mass flux balance will be discussed in Section 4.

The right hand side terms in the kinetic stress equation (7) are, respectively, viscous dissipation due to drag against the background gas, divergence of the turbulent energy flux, "P-dV work" (expansion or compression work) and finally a source $\bar{\mu}$ due to the turbulent forcing of the particles. It is interesting to see that the stress equation is similar to a normal single phase *gas energy* conservation equation. The new features are the dissipative drag term and the turbulent source – both reflecting the interaction with the background fluid. In homogeneous stationary turbulence, the kinetic stress equation simply reduces to a statement of local balance between the dissipation and turbulent source from which E_z follows. In inhomogeneous turbulence with zero mean velocity (as we will encounter below), we get an additional contribution from the energy flux divergence which gives non-local coupling. The particular form of the energy flux, $F_z = -\rho\epsilon_{zz}\partial_z E_z$, is a consequence of the Chapman–Enskog closure relation applied to the associated triple velocity correlation (e.g., Swailes et al., 1998). We also note that the energy flux is non-linear in the kinetic stress.

2.3. Stationary solution with zero mass flux normal to the boundaries

We will in the following consider a stationary situation in which the particle distribution and fluid turbulence is fully developed and where the net mass flux normal to the boundaries is zero. The (normal mean) velocity within the domain vanishes ($\bar{v}_z = 0$), and the momentum equation reduces to one of "hydrostatic" balance

$$\partial_z T_{zz} = -(g + \bar{\gamma}_z)\rho = -g_{\mathrm{eff}}\rho, \tag{12}$$

where the effective gravity is $g_{\mathrm{eff}} = g + \bar{\gamma}_z$. This is the same as that of a normal stratified gas, with T_{zz} replaced by the gas pressure P, and g_{eff} by g. The momentum equation can be integrated directly by using the general relation $T_{zz} = \beta\rho\epsilon_{zz} = (\rho\epsilon_{zz})/\tau_{\mathrm{p}}$

$$\frac{\mathrm{d}T_{zz}}{T_{zz}} = -\frac{g_{\mathrm{eff}}\rho}{T_{zz}}\,\mathrm{d}z = -\frac{g_{\mathrm{eff}}\tau_{\mathrm{p}}}{\epsilon_{zz}}\,\mathrm{d}z,$$

giving

$$\rho(z) = \rho(0)\frac{\epsilon_{zz}(0)}{\epsilon_{zz}(z)}\exp\left\{-\tau_{\mathrm{p}}\int_0^z \frac{g_{\mathrm{eff}}}{\epsilon_{zz}}\,\mathrm{d}z\right\}. \tag{13}$$

This is a general reformulation of the momentum equation and will therefore also account fully for turbophoresis via the variation of the diffusivity $\epsilon_{zz}(z) = \tau_{\mathrm{p}}(2E_z + \bar{\lambda}_{zz})$ with height.

A solution of the problem in terms of $\rho(z)$ will require solving the stress equation for E_z. In the stationary case with zero mass flux, the stress equation reduces to

$$2\beta\rho E_z = \partial_z(\rho\epsilon_{zz}\partial_z E_z) + \rho\bar{\mu}_{zz}. \tag{14}$$

Combining this with the momentum equation gives a *single equation* for E_z, in the form of the non-linear second order equation

$$2\beta^2 E_z + g_{\text{eff}}\partial_z E_z - (2E_z + \bar{\lambda}_{zz})\partial_z^2 E_z = \beta\bar{\mu}_{zz}. \tag{15}$$

The two required boundary conditions are chosen as the two endpoint values of the normal stress E_z. A solution is obtained by linearization and Newton–Raphson iteration. The linearized differential equation corresponds to a tridiagonal matrix equation which is easy to implement numerically. The initial guess can be taken as the homogeneous value, $(E_z)_{\text{hom}} = (\bar{\mu}_{zz})_{\text{hom}}/(2\beta)$.

The solution procedure then starts with solving Eq. (15) for the kinetic stress, by providing two boundary conditions. The integral form of the momentum equation (13) can then be solved with a boundary condition for the density (e.g., the lower endpoint value).

2.4. Equilibrium dispersion tensors in stationary turbulence

The long time equilibrium dispersion tensors are obtained by assuming that the time since release of the particle into the flow is sufficiently long such that the initial particle momentum has no influence. The particle has then reached an "equilibrium" with the background flow. This is reasonable a few mean free paths $v_0\tau_{\text{p}}$ away from the boundaries, where v_0 is the characteristic particle injection velocity at the boundary (in our case, v_0 is the velocity boundary condition for the PT-scheme).

2.4.1. Tensor components for the 1D stationary case

The (z,z) component of the velocity averaged dispersion tensors are

$$\bar{\mu}_{zz}(z) = \langle \Delta v_z(z,t) f_z'(z,t)\rangle, \tag{16}$$

$$\bar{\lambda}_{zz}(z) = \langle \Delta z(z,t) f_z'(z,t)\rangle, \tag{17}$$

$$\bar{\gamma}_z(z) = -\langle \Delta x_j(z,t)\partial_{x_j} f_z'(z,t)\rangle = -\langle (\Delta\mathbf{x}(z,t)\cdot\nabla) f_z'(z,t)\rangle. \tag{18}$$

The displacements Δv_z and Δz now refer to all particle trajectories arriving at z irrespective of their velocity (note that in the stationary case the dispersion tensors do not vary with time). This form is sufficient for calculating the dispersion tensors directly from the PT simulations. However, to gain more insight we need to express the dispersion tensors explicitly in terms of the correlation function of the fluctuating force. Green's function for the displacement Δz, considering drag only, is

$$g(t;s) = \beta^{-1}(1 - \mathrm{e}^{-\beta(t-s)}), \tag{19}$$

where s is the source time. The displacement due to the random force is the accumulated effect over the particle path

$$\Delta x_j = \int_{t_1}^{t} f_j'(z,t;s) g(t;s)\,\mathrm{d}s. \tag{20}$$

The accumulated velocity from the same random force is

$$\Delta v_j = \int_{t_1}^{t} f_j'(z,t;s)\dot{g}(t;s)\,\mathrm{d}s, \tag{21}$$

where $\dot{g}(t;s) = \mathrm{e}^{-\beta(t-s)}$. From these expressions, we obtain

$$\bar{\mu}_{zz}(z) = \int_{t_1}^{t} \langle f_z'(z,t) f_z'(z,t;s)\rangle \dot{g}(t;s)\,\mathrm{d}s,$$

$$\bar{\lambda}_{zz}(z) = \int_{t_1}^{t} \langle f_z'(z,t) f_z'(z,t;s)\rangle g(t;s)\,\mathrm{d}s,$$

$$\bar{\gamma}_z(z) = -\int_{t_1}^{t} \langle f_j'(z,t;s)\partial_{x_j} f_z'(z,t)\rangle g(t;s)\mathrm{d}s,$$

where angle brackets enclose forms of the Lagrangian force correlation function (in the sense of following a particle, and not a fluid element). Summation over the index j is performed in the expression for $\bar{\gamma}_z$. The force

depends on the time s, and therefore on the particle path history. In homogeneous turbulence, it does not matter where the particle has been due to statistical homogeneity, and one can evaluate the dispersion tensors exactly given a specific form of the temporal correlation function. One usually adopts an exponential correlation function in the case of homogeneous turbulence,

$$\langle u_i'(z,t)u_j'(z,t;s)\rangle = \langle u_i u_j\rangle \mathrm{e}^{-|t-s|/\tau}, \tag{22}$$

with a spatially uniform correlation time τ. One of the goals below is to evaluate the dispersion tensors in inhomogeneous turbulence where the particle paths have to be accounted for.

It is here appropriate to mention the influence of fluid shear on the dispersion tensors. With a constant shear $S_{z,x} = \partial_z\langle u_x\rangle$, the dispersion tensors in *homogeneous* turbulence are (e.g., Reeks, 1993, 2005)

$$(\bar{\lambda}_{ij})_{\mathrm{hom}} = \langle u_i u_j\rangle \frac{(\beta\tau)^2}{1+\beta\tau} + \delta_{x,i}\tau S_{z,x}\langle u_j u_z\rangle \frac{(\beta\tau)^3}{(1+\beta\tau)^2},$$

$$(\bar{\mu}_{ij})_{\mathrm{hom}} = \frac{(\bar{\lambda}_{ij})_{\mathrm{hom}}}{\tau},$$

$$(\bar{\gamma}_i)_{\mathrm{hom}} = 0.$$

We note that shear has no influence on the (z,z) components which are used in the 1D continuum equations. We will assume that this also holds for a non-linear mean velocity profile (i.e., varying shear) in *inhomogeneous* turbulence.

2.4.2. The passive scalar approximation (PSA) for $\bar{\gamma}_i$

The analysis of Swailes and Darbyshire (1999) and Reeks (1992), shows indirectly that in the passive scalar limit ($\tau_{\mathrm{p}} \to 0$), one can relate $\bar{\gamma}_i$ directly to $\bar{\lambda}_{ij}$, when we impose that the density should be constant in the limit ("well mixed condition"). The well mixed condition will be accounted for in the PT-simulation by adding a correction term to the Langevin equation to counteract spurious drift (Thomson, 1984).

In the limit $\tau_{\mathrm{p}} \to 0$, the leading order terms in the momentum equation must balance, giving

$$\rho\bar{v}_i \to \rho\langle u_i\rangle + \tau_{\mathrm{p}} j_i, \tag{23}$$

where the velocity averaged diffusion current is

$$j_i(\mathbf{x},t) = -\nabla\cdot(\langle \mathbf{\Delta x} f_i'\rangle\rho) - \bar{\gamma}_i\rho \tag{24}$$

and where ρ approaches the density of passive tracers ρ_{f}. Then, for known velocity and density of the passive tracer, Eqs. (23) and (24) define an inhomogeneous differential equation relating $\bar{\lambda}_{ij}$ and $\bar{\gamma}_i$.

In the current case of zero mass flux (and zero mean fluid velocity) perpendicular to the walls, the z-component of (24) reduces to

$$\partial_{x_j}(\bar{\lambda}_{jz}\rho) + \bar{\gamma}_z\rho = 0.$$

In stratified, fully developed stationary turbulence, there is no variation of ensemble averaged quantities in the horizontal plane such that $\partial_x(\bar{\lambda}_{xz}\rho) = \partial_y(\bar{\lambda}_{yz}\rho) = 0$, and in that case the following equation relates the two dispersion tensors:

$$\partial_z(\bar{\lambda}_{zz}\rho) + \bar{\gamma}_z\rho = 0. \tag{25}$$

If we further impose constant density (well mixed condition), the two dispersion tensors are directly related via the equation

$$\bar{\gamma}_z = -\partial_z\bar{\lambda}_{zz}. \tag{26}$$

In other terms, (26) is the condition to be imposed on the tensor components in question in the limit $\tau_{\mathrm{p}} \to 0$ for a well mixed 1D stationary flow with zero mass flux. I will use (26) as an approximation (PSA – passive scalar approximation) also in the case of "light inertial particles" for which $\tau/\tau_{\mathrm{p}} \gg 1$ (small Stokes number). We note that the PSA form accounts approximately for the gradient in turbulence intensity while the strict LHA form does not.

For further comparison to Swailes and Darbyshire (1999) and Reeks (1992), it is convenient to rewrite the 1D momentum equation as a diffusion equation expressing the different mass flux contributions. In the 1D stationary case and for all τ_p, the perpendicular mass flux is generally

$$\rho\bar{v}_z = -\tau_p\rho\frac{D\bar{v}_z}{Dt} - \tau_p\partial_z(2E_z) - \tau_p\rho(\partial_z\bar{\lambda}_{zz} + \bar{\gamma}_z) - \rho\tau_p g - \epsilon_{zz}\partial_z\rho. \tag{27}$$

This diffusion equation is the 1D version of that in Reeks (1992) (his equation 77), except that gravity is added. In the limit $\tau_p \to 0$ (or $\beta\tau = \tau/\tau_p \gg 1$), $\bar{\lambda}_{zz} \to \infty$ and $\epsilon_{zz} \to \tau_p\bar{\lambda}_{zz}$ approaches a finite value corresponding to the fluid diffusivity. Thus

$$\rho\bar{v}_z \to -\tau_p\rho(\partial_z\bar{\lambda}_{zz} + \bar{\gamma}_z) - \tau_p\bar{\lambda}_{zz}\partial_z\rho = -\tau_p(\partial_z[\rho\bar{\lambda}_{zz}] + \rho\bar{\gamma}_z), \tag{28}$$

which is consistent with (25) for zero mass flux. Finally, it is noted that Devenish et al. (1999) used a PSA-like approximation also for higher inertia particles in inhomogeneous turbulence. Without giving a rigorous justification, they adopted a constant (characteristic) $\tau = \tau_f$ and the relation

$$\bar{\gamma}_z = -\bar{\lambda}_{zz}\partial_z \ln\sigma_u^2, \tag{29}$$

(in the current notation with $\kappa = -\bar{\gamma}_z$). Here, σ_u is the normal component of the turbulence intensity. This relation is in fact a special case of (26), by adopting the LHA form of λ_{zz} with a constant τ.

2.5. Particle tracking in Langevin turbulence

The vertical component of the linear equations of motion for a single massive particle is in general

$$\dot{v}(t) = \beta\{u[x(t), y(t), z(t)] - v(t)\} - g, \tag{30}$$

$$\dot{z}(t) = v(t), \tag{31}$$

where u is the vertical component of the background fluid velocity on the path $[x(t), y(t), z(t)]$ of the particle. In inhomogeneous turbulence, the statistics of u in terms of intensity σ_u and integral timescale τ will vary with position. In the current 1D problem, these parameters vary only with z. It is then not necessary to assign horizontal coordinates $[x(t), y(t)]$ to u, and the vertical component of the equation of motion is sufficient information.

Following Iliopoulos and Hanratty (1999) and Mito and Hanratty (2002, 2005) the turbulent fluid velocity $u(z(t))$ is modeled by the Langevin equation in the normalized variable $Y(t) = u(z(t))/\sigma_u(z(t))$

$$dY(t) = -\frac{Y(t)}{\tau(z(t))}\,dt + \partial_z\sigma_u(z(t))\,dt + d\zeta(t), \tag{32}$$

$$\langle(d\zeta)^2\rangle = \frac{2}{\tau(z(t))}\,dt, \tag{33}$$

where $d\zeta$ is white noise with variance $\langle(d\zeta)^2\rangle$. The signal $u(z(t))$ can be regarded as "colored" noise with a certain local correlation time $\tau(z(t))$ and local variance $\sigma_u^2(z(t))$. The drift term $\partial_z\sigma_u dt$ is introduced to counteract "spurious drift" associated with Langevin turbulence modeling (Thomson, 1984). This ensures constant particle density in the passive tracer limit (sometimes referred to as the "well mixed condition").

The equations above are discretized according to the Adams–Bashforth scheme. For velocity and position a second-order explicit Adams–Bashforth scheme is used. For the Langevin equation, the Adams–Bashforth–Moulton third-order implicit scheme involving iterations is used. The iterations are stopped after 3–4 iterations giving an accuracy better than second order, but worse than third order. The given timescale $\tau(z)$ and intensity $\sigma_u(z)$ are sampled using linear interpolation at $z(t)$.

Since the problem is defined to be stationary without inter-particle collisions, a single particle is followed over a long period of time to obtain the necessary statistics. When the particle intersects one of the boundaries, it is injected back into the domain with a velocity taken from a specific distribution. In this way, we ensure that the mass flux at the boundaries as well as in the interior is zero. The domain is divided into bins of size Δz, centered at positions z_k. The number of occurrences in a certain bin k represents the particle concentration at

z_k. The mean velocity (zero in our case) and velocity variance (normal kinetic stress) as function of z_k are obtained by recording the velocities in bin k.

2.6. Specification of the fluid turbulence, normalization and parameter settings

The timescale τ is neither the Lagrangian τ_L nor the Eularian τ_E integral timescale. In the absence of gravity, Reeks (1977) shows that $\tau_L < \tau < \tau_E$ with τ approaching the Lagrangian timescale for $\tau_p \to 0$ and the Eulerian timescale for $\tau_p \to \infty$. When gravity is imposed, τ may be smaller than τ_L since the particle transit time over a "turbulent eddy" can be reduced. Csanady (1963) arrived at a formula for the particle diffusivity under gravitational drift in a homogeneous turbulent medium. We will ignore this gravitational "crossing trajectories" effect in the current work, and simply assume the relation $\tau \simeq \tau_L$.

In order to derive an approximate relation for τ_L which relates to standard turbulence parameters, we first consider the normal component of the passive scalar diffusivity in homogeneous turbulence

$$(\epsilon_{zz})_h = \langle u_z' u_z' \rangle \tau_L. \tag{34}$$

We adopt this form locally in *inhomogeneous* turbulence, and propose in addition that $(\epsilon_{zz})_h \simeq \nu_T$ where ν_T is the eddy viscosity. The applied formula is, therefore

$$\tau_L \simeq \frac{\nu_T}{\langle u_z' u_z' \rangle}, \tag{35}$$

where one may adopt the algebraic eddy viscosity model of Biberg (2005). For single phase channel flow the dimensionless Biberg eddy viscosity reduces to the Poiseuille form

$$\nu_T = \frac{\kappa Z(1-Z)(1-3Z(1-Z))}{1-Z(1-Z)}, \tag{36}$$

where $Z \in [0,1]$ is the normalized coordinate between the walls, and κ is von Kármán's constant. For the normal component of the turbulent intensity $\sigma_u = \sqrt{\langle u_z' u_z' \rangle}$, we will use the Altunbaş et al. (2002) formula for pipe flow valid in the range $4 \times 10^4 < Re < 5 \times 10^5$. In normalized form, this reads

$$\sigma_u = 0.72[1 - e^{-6.25Z} + 4.46\sqrt{Z}e^{-7.49Z}] \tag{37}$$

for $Z \in [0, 1/2]$ (and a reversed profile for the remaining interval $Z \in [1/2, 1]$). The resulting timescale

$$\tau \equiv \nu_T/\sigma_u^2 \tag{38}$$

is qualitatively similar to that used in the PT-simulations of Mito and Hanratty (2002, 2005) such that the results below will be comparable to their work. We note that τ can also be expressed in terms of σ_u and the dissipation rate of turbulence energy (e.g., Mito and Hanratty, 2002). The accuracy of (38) is not very important in the following, since we will be mostly concerned with the differences between kinetic theory and the PT-data given the same parameters τ and σ_u.

Following Mito and Hanratty (2005), the characteristic velocity is the friction velocity $v_c = v^*$ and the characteristic time scale is $t_c = \nu/(v^*)^2$ where ν is the kinematic viscosity of the carrier fluid. The characteristic length scale is $l_c = v_c t_c = \nu/v^*$. All quantities are normalized to these scales in the following, and the '+' notation is omitted throughout. The parameter settings of Mito and Hanratty (2005) is applied, where the relaxation time is $\tau_p = 20$ and the terminal velocity is $g\tau_p = 0.12$. The injection velocity at the boundaries is $V = \pm 1$ (corresponding to a delta function distribution for velocities into the domain) to reproduce the Mito and Hanratty-simulation. Once a particle hits the boundary from the interior, it is injected back into the flow with $V = +1$ at the lower boundary and $V = -1$ at the upper boundary. The boundary is therefore not a purely reflective one.

3. Results

In the regime of $\beta\tau = \tau/\tau_p \gg 1$, all the dispersion tensors $\bar{\gamma}$, $\bar{\lambda}$ and $\bar{\mu}$ have significant impact on the continuum equation solutions. Inaccurate estimates of these tensors can then lead to large errors. The local mean

free path $\sqrt{2E_z}\tau_p$ in the bulk flow approaches zero in this regime and one might therefore expect that the LHA form of the dispersion tensors would be a reasonable closure relation (e.g., Reeks, 1992). However, it is demonstrated below that this is not necessarily the case.

It is interesting that in the opposite regime of high inertia particles, $\beta\tau \ll 1$, one can neglect $\bar{\gamma}$ and $\bar{\lambda}$ in comparison to $\bar{\mu}$ and inaccurate estimates of $\bar{\gamma}$ and $\bar{\lambda}$ may be irrelevant for the final result[2] (recalling that in this case the LHA form of these dispersion tensors should be invalid due to the larger particle mean free path). In that case, however, we expect that the Chapman–Enskog closure relation for the energy flux breaks down, and the final results may still be in error for this reason.

There will be a zone near the boundaries where the particles relax from the injection condition to the background turbulence. To ensure that the use of long-time dispersion tensors is a valid approach, the KT continuum equations are solved between two *internal boundaries*, a few mean free paths away from the injection points in the PT-simulation. The density and kinetic stress from the PT-simulation are taken as boundary conditions for the continuum equations. See Fig. 1. In particular, the two endpoint values of kinetic stress are used for Eq. (15). The lower endpoint value of the density is taken as a boundary condition of the integral form of the momentum Eq. (13). With the timescale τ defined above, we work in the regime $\beta\tau = \tau/\tau_p \in [1, 5]$, with the smaller ratio near the boundaries of the continuum calculation.

3.1. PSA versus LHA for $\bar{\gamma}_z$

In LHA, one simply adopts the homogeneous form of the dispersion tensors

$$(\bar{\lambda}_{zz})_{\text{hom}} = \langle u_z u_z \rangle \frac{(\beta\tau)^2}{1+\beta\tau},$$

$$(\bar{\mu}_{zz})_{\text{hom}} = \frac{(\bar{\lambda}_{zz})_{\text{hom}}}{\tau},$$

$$(\bar{\gamma}_z)_{\text{hom}} = 0,$$

where spatially local values of $\langle u_z u_z \rangle$ and τ are inserted. The smooth thick lines in the left panel of Fig. 2 shows the continuum solutions for density (concentration) and normal stress using the homogeneous forms of the dispersion tensors. The thin jagged lines are the corresponding ensemble averages from the particle simulation. It is seen that the concentration profile from kinetic theory is in severe error, indicating an imbalance in the momentum equation due to the LHA form $\bar{\gamma}_z = 0$.

The particle kinetic stress (thick line in the right panel in Fig. 2) fits the PT results quite well, suggesting that the LHA form of $\bar{\mu}_{zz}$ is sufficiently accurate. We note that $\bar{\mu}_{zz}$ provides the source in the kinetic stress equation (15). The dashed line shows the locally homogeneous approximation for the kinetic stress, resulting from ignoring the energy flux (the Chapman–Enskog closure relation). The corresponding result is virtually indistinguishable from the KT-result (thick line), showing that there is a near balance between generation and dissipation of kinetic energy. One should note that the magnitude of the Chapman–Enskog term depends on the concentration (density) gradient and the particle relaxation time, and should not be neglected a priori. Furthermore, we expect that this term can be more significant for particles with larger relaxation time ($\tau_p/\tau \sim 1$ or larger), and in particular in boundary layers where there are strong gradients in turbulence intensity of the fluid.

In Fig. 3, the PSA form of $\bar{\gamma}_z$ is used

$$(\bar{\gamma}_z)_{\text{PSA}} = -\partial_z(\bar{\lambda}_{zz})_{\text{hom}},$$

keeping the LHA forms $(\bar{\lambda}_{zz})_{\text{hom}}$ and $(\bar{\mu}_{zz})_{\text{hom}}$. It is evident from the figure that the concentration profile is improved, giving a better prediction of the PT result, but it is still not fully satisfactory.

From the right panel in Fig. 3, we see again that the solution for the kinetic stress is acceptable. The remaining discrepancy in concentration must then be attributed to inaccuracy in $(\bar{\lambda}_{zz})_{\text{hom}}$ or to the fact that

[2] In this regime, the Liouville equation reduces to a Fokker–Planck equation.

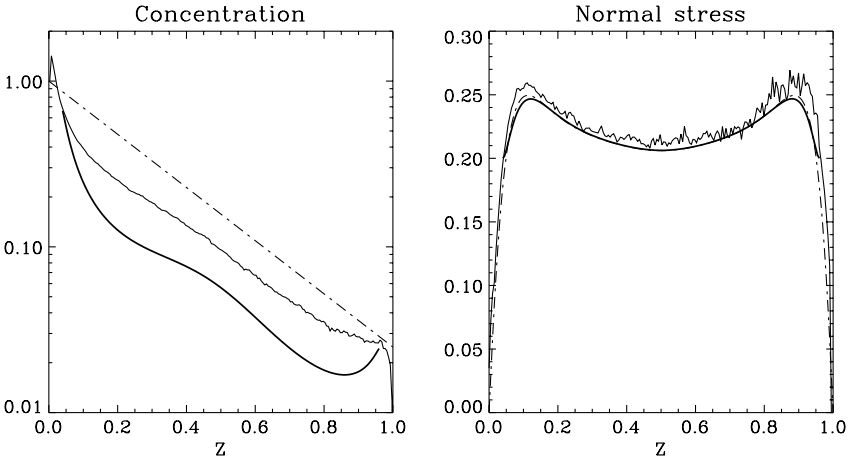

Fig. 2. *Concentration and normal stress using LHA dispersion tensors.* Mito and Hanratty case with $\tau_p = 20$, $V_t = 0.12$. Thin full lines: Ensemble averaged PT-simulation. Thick lines: continuum equations. Z is the normalized coordinate between the walls. *Left panel:* Normalized concentration profiles. Dashed line: First order approximation corresponding to the mean density scale height. *Right panel:* Normal stress $\overline{v_z' v_z'}$. Dashed line: Locally homogeneous approximation (ignoring the Chapman–Enskog energy flux).

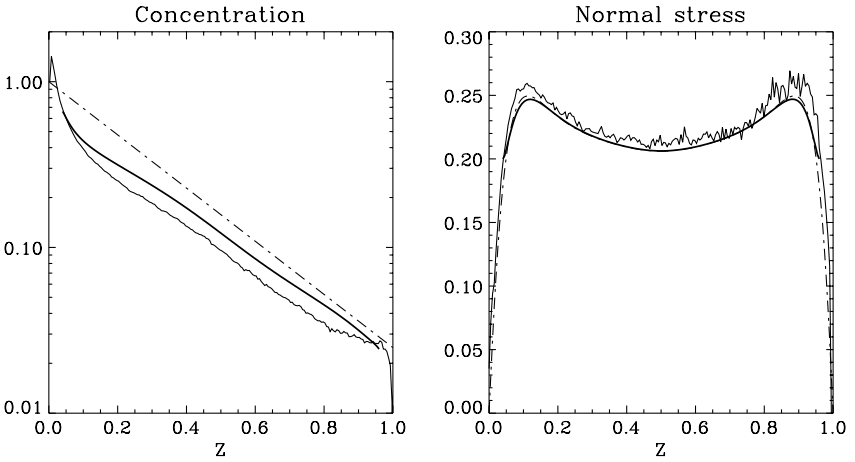

Fig. 3. The PSA form of $\bar{\gamma}_z$ is applied in the momentum equation. The LHA form of $\bar{\lambda}_{zz}$ and $\bar{\mu}_{zz}$ is kept. The line styles coding and the physical parameters are the same as for Fig. 2.

the PSA-relation is only approximate. In the next section it is shown that the PSA holds, while the exact $\bar{\lambda}_{zz}$ evaluated from the PT-simulation differs from $(\bar{\lambda}_{zz})_{\mathrm{hom}}$.

3.2. Direct evaluation of the dispersion tensors $\bar{\lambda}_{zz}$ and $\bar{\mu}_{zz}$ using PT-data

The dispersion tensor component $\bar{\lambda}_{zz}$ is in general given by the ensemble average

$$\bar{\lambda}_{zz}(z) = \langle f_z'(z,t)\Delta z(z,t)\rangle, \tag{39}$$

where Δz is the displacement of the particle due to the turbulent force. This can be evaluated directly in the PT simulation by recording the force f_z' on the particle when it passes the evaluation point z. The displacement $\Delta z(t) = z - z(t_0)$ is recorded by measuring the particle position at time t_0 which should be chosen such that $t - t_0$ is much larger than the characteristic fluid integral timescale τ_{char} that the particle experiences along

the path. Only the force within the time interval $t - t_0 \leqslant \tau_{\text{char}}$ will contribute significantly to the portion of the displacement which correlates to f_z'. Similarly, the dispersion tensor component $\bar{\mu}_{zz}$ is in general given by

$$\bar{\mu}_{zz}(z) = \langle f_z'(z,t)\Delta v(z,t)\rangle, \tag{40}$$

where $\Delta v(z,t)$ is the recorded change in velocity.

The upper two panels in Fig. 4 show the resulting dispersion tensors. The crosses show $\bar{\lambda}_{zz}$ and the triangles show $\bar{\mu}_{zz}$ as functions of Z. The thin lines show the locally homogeneous versions (LHA) which are necessarily symmetric about the midpoint of the domain. For later use in the continuum equations, the evaluated dispersion tensors where fitted with smooth functions (fits to the crosses and triangles). These fits are also shown in Fig. 4. The most notable feature is that $\bar{\lambda}_{zz}$ deviates significantly relative to the LHA version with a pronounced skew towards the upper boundary, while $\bar{\mu}_{zz}$ does not deviate very much from the LHA version.

The smooth fits to the PT-evaluated $\bar{\lambda}_{zz}$ and $\bar{\mu}_{zz}$ are then inserted into the continuum equations to generate solutions which should match the PT-data. Again, the PSA-relation for $\bar{\gamma}_z$ is adopted. The corresponding results are compared to the PT-data in Fig. 5. It is clear that the concentration profile is improved compared

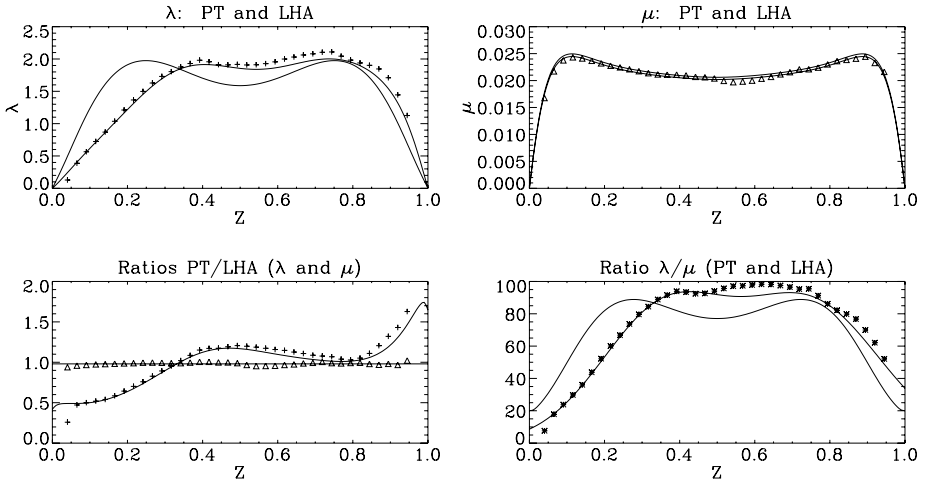

Fig. 4. *Dispersion tensors evaluated from PT-data. Upper panels:* The crosses (left) show $\bar{\lambda}_{zz}$ and triangles (right) show $\bar{\mu}_{zz}$ as functions of Z. The thin lines show the locally homogeneous versions (LHA) and smooth functional fits to the evaluated dispersion tensors. *Lower left panel:* The ratios $[\bar{\lambda}_{zz}]_{\text{PT}}/[\bar{\lambda}_{zz}]_{\text{LHA}}$ and $[\bar{\mu}_{zz}]_{\text{PT}}/[\bar{\mu}_{zz}]_{\text{LHA}}$ are plotted to further evaluate the quality of the smoothed fits (thin lines denote the corresponding smoothed fit ratio). *Lower right panel:* The ratios $[\bar{\lambda}_{zz}/\bar{\mu}_{zz}]_{\text{PT}}$ and $[\bar{\lambda}_{zz}/\bar{\mu}_{zz}]_{\text{LHA}} = \tau(z)$.

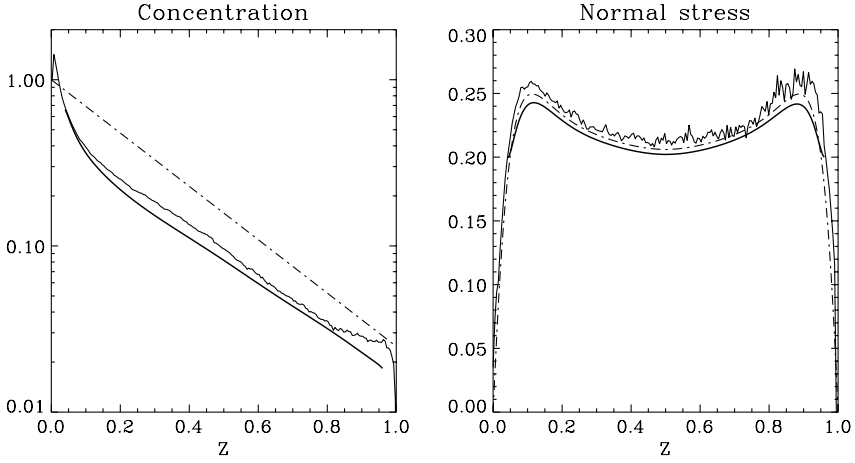

Fig. 5. *PSA for $\bar{\gamma}_z$ with $\bar{\lambda}_{zz}$ and $\bar{\mu}_{zz}$ calculated from the PT-data.* The line styles and the physical parameters are the same as for Fig. 2.

to Fig. 3, where the LHA value of $\bar{\lambda}_{zz}$ was used. The kinetic stress from the continuum equation is still acceptable, although we see a few percent under-prediction relative to the PT-data (right panel). In this respect, we note that the kinetic stress depends on both $\bar{\lambda}_{zz}$ and $\bar{\mu}_{zz}$ (cf. Eq. 15) such that a significant change of $\bar{\lambda}_{zz}$ may also affect the kinetic stress.

3.3. The non-local nature of $\bar{\lambda}_{zz}$ and the particle diffusivity ϵ_{zz}

The most important results above are that the LHA version of $\bar{\mu}_{zz}$ is a good approximation, while the LHA version of $\bar{\lambda}_{zz}$ is not. This can be understood by considering the differences in the Green's functions for displacement and velocity. As shown previously, the component $\bar{\lambda}_{zz}$ is proportional to the integral of $\langle u(z,t)u(z(s),s)\rangle g(t;s)$ over the time parameter $s < t$ (recalling that $f_z' = \beta u$). Since $g \rightarrow 0$ for $s \rightarrow t$ with $1/e$ time equal to τ_p, and $\tau/\tau_p \gg 1$ in the current regime, it is the "effective" correlation time τ_{char} of $\langle u(z,t)u(z(s),s)\rangle$ which determines the support of the integrand along the time axis. These considerations are further illustrated in the left panel of Fig. 6, which shows the contributions to the dispersion tensors at normalized height $Z = 0.3$. The parameters were again $\tau_p = 20$ and $V_t = 0.12$.

In the case of $\bar{\mu}_{zz}$, the integrand in question is $\langle u(z,t)u(z(s),s)\rangle \dot{g}(t;s)$ where $\dot{g}(t;s) \rightarrow 0$ for increasing $|s-t|$, again with $1/e$ time equal to τ_p. In the same regime ($\tau/\tau_p \gg 1$), it is then the shorter particle relaxation time τ_p (rather than τ_{char}) which defines the time support of the integrand (right panel of Fig. 6). In the case studied, the corresponding averaging volume is sufficiently small that $\bar{\mu}_{zz}$ is close to the LHA-value.

The correlation function $\langle u(z,t)u(z(s),s)\rangle$ depends on an average measure of $\tau(z)$ and $\sigma_u(z)$ over a volume spanned by the particle paths converging onto the evaluation point z. In 1D, the corresponding interval $D(t-s)$ (say, defined by the RMS spread of the paths) is time dependent and shrinking as illustrated in Fig. 7. One would expect that if $D(\tau_{char}) > l_{turb}$ where l_{turb} is the characteristic length scale of the turbulence parameters (σ_u and τ), then $\bar{\lambda}_{zz}$ is sensitive to turbulence inhomogeneity. A rough criterion for when the LHA form of $\bar{\lambda}_{zz}$ is valid may then be derived by adopting the long-term dispersion formula in homogeneous turbulence

$$D(z,t-s) \simeq \sqrt{2\epsilon_{zz}(z)(t-s)}. \tag{41}$$

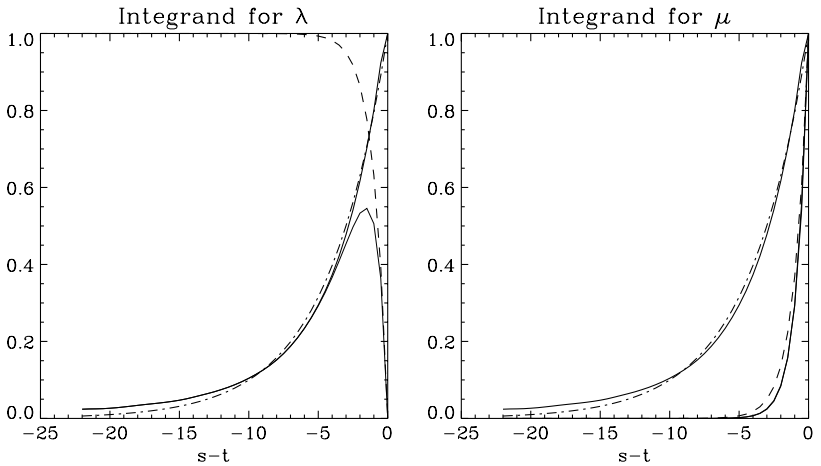

Fig. 6. *Contributions to the dispersion tensor integrands at Z = 0.3.* Thin line: Velocity correlation function $\langle u(z,t)u(z(s),s)\rangle$ from the PT-simulation, as a function of the time difference $(s-t)$ normalized to τ_p. This correlation function is characterized by the "effective" correlation time τ_{char}. The dash-dot line shows the exponential $\exp(-(t-s)/\tau(z))$ with local integral timescale $\tau(z)$ at the evaluation point. Dashed line: Weight corresponding to the particular Green's function in question. Note that for large $|t-s|$ the weight for $\bar{\lambda}_{zz}$ approaches unity while the weight for $\bar{\mu}_{zz}$ approaches zero. Thick line: Integrand (Green's function weight times the velocity correlation function) for $\bar{\lambda}_{zz}$ (left panel) and $\bar{\mu}_{zz}$ (right panel). It is seen that $\bar{\lambda}_{zz}$ is more dependent on the particle path history (and therefore turbulence inhomogeneity) than $\bar{\mu}_{zz}$.

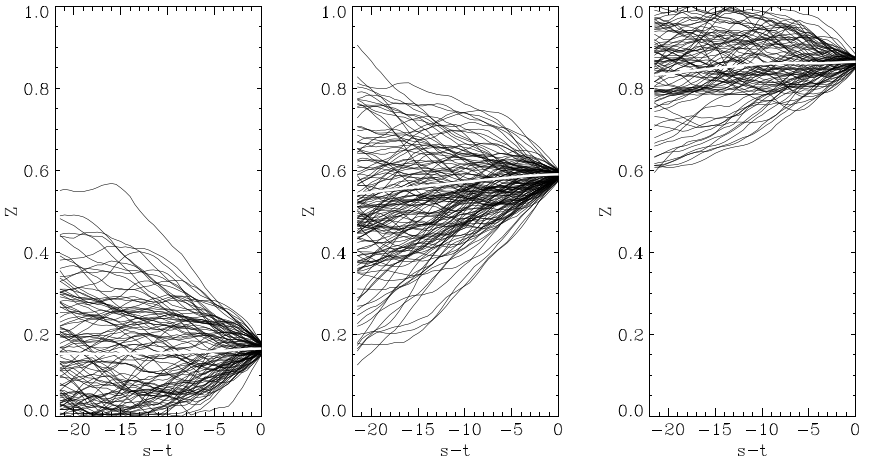

Fig. 7. A few selected particle paths conditional on intersection at the particular evaluation points $z = 0.15, 0.55, 0.85$. Thick white lines: Corresponding mean path. Time is here in units of τ_p.

If we use the locally homogeneous diffusivity $\epsilon_{zz} \simeq \sigma_u^2\tau$, the suitable "LHA criterion" $D(\tau_{\text{char}}) \ll l_{\text{turb}}$ translates to $\sigma_u\tau \ll l_{\text{turb}}$ (or $l_{\text{eddy}} \ll l_{\text{turb}}$). With our definition of τ, this criterion can also be written $v_T \ll \sigma_u l_{\text{turb}}$.

In the limit $\tau_p \to 0$ corresponding to passive tracers co-moving with the fluid-particles, the contribution to diffusion from kinetic stress vanishes and the particle diffusivity ϵ_{zz} approaches the value of the fluid diffusivity ϵ_F

$$\epsilon_{zz} \to \tau_p\bar{\lambda}_{zz} \to \epsilon_F = \int_{-\infty}^{t} \langle u(z,t)u(z(s),s)\rangle \,\mathrm{d}s = \langle u(z,t)\Delta z_f(z,t)\rangle, \tag{42}$$

where Δz_f is the displacement corresponding to a realization of a fluid trajectory $z(s)$. We note that this integral form is identical to the expression for the classical fluid diffusivity in homogeneous turbulence (e.g., Taylor, 1921; Kraichnan, 1970). In inhomogeneous turbulence, it is clear that even the fluid diffusivity ϵ_F depends on the turbulence characteristics in the volume surrounding the evaluation point. Thus, a locally homogeneous approximation for the fluid diffusivity, such as $\sigma_u^2(z)\tau(z) = \epsilon_f$, may not be a valid substitute for ϵ_F in (42) in inhomogeneous turbulence.

4. Mass flux balance

Mito and Hanratty (2005) tested the widely used diffusion equation model

$$v_d\rho - \epsilon_f\partial_z\rho = 0 \tag{43}$$

against PT-simulations, where v_d is a general drift velocity (terminal velocity plus turbophoretic drift). A *local* approximation to the fluid diffusivity $\epsilon_f(z)$ was regarded as a good approximation to the actual particle diffusivity, although this may not be justified in inhomogeneous turbulence even for passive tracers as shown above. These authors found an imbalance between the mass flux terms when these were evaluated using PT-data. One is therefore led to the conclusion that such a model cannot fully capture the physics of the problem. This is an important observation since this type of phenomenological model is still widely used in applications.

The diffusion equation built on the KT continuum momentum equation reads

$$\tau_p\rho\partial_z\overline{v_z'v_z'} + \tau_p\rho\partial_z\bar{\lambda}_{zz} + \epsilon_{zz}\partial_z\rho + \rho g_{\text{eff}}\tau_p = 0. \tag{44}$$

Within the PSA, the additional term in $\partial_z\bar{\lambda}_{zz}$ cancels $\bar{\gamma}_z$ in g_{eff}. After dividing (44) by density, and invoking PSA, we obtain the drift velocity balance

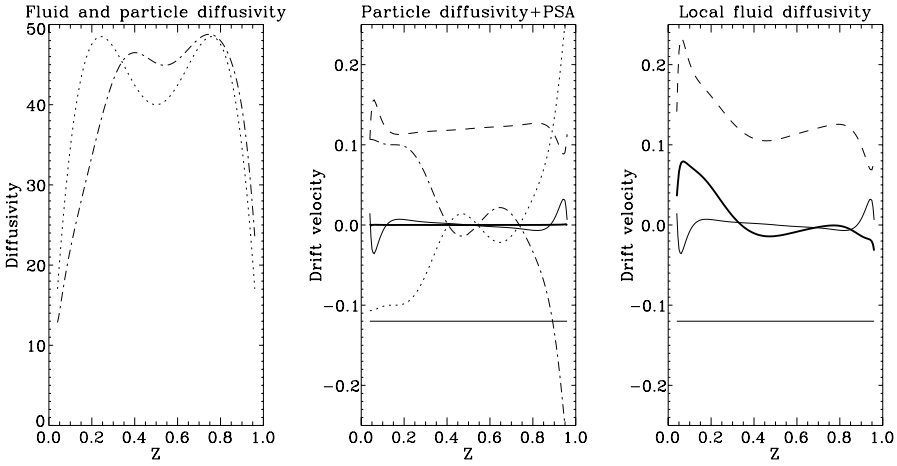

Fig. 8. *Left panel:* Local approximation to the fluid diffusivity (dots) and kinetic theory particle diffusivity (dash-dots). *Middle and right panels:* Drift velocities in the diffusion Eq. (45), with $\tau_p = 20$ and $V_t = 0.12$. Thick lines: residual after adding all drift velocity contributions. Dashed line: diffusive velocity $-\epsilon_{zz}\partial_z(\ln(\rho))$. Full line: turbophoresis $-\tau_p\partial_z\overline{v_z'v_z'}$. Full straight line: settling velocity $-g\tau_p$. *Middle panel:* The terms $-\tau_p\bar{\gamma}_z$ (dash-dots) and $-\tau_p\partial_z(\bar{\lambda}_{zz})$ (dots) cancel due to the adopted PSA-relation leading to (45). *Right panel:* The balance from using the local fluid diffusivity rather than the particle diffusivity. Only the diffusive velocity is altered (dashed line).

$$-g\tau_p - \tau_p\partial_z\overline{v_z'v_z'} - \epsilon_{zz}\partial_z \ln\rho = 0. \tag{45}$$

We recognize $-g\tau_p$ as the terminal velocity (gravitational drift velocity) and $-\epsilon_{zz}\partial_z\ln\rho$ is the drift velocity associated with turbulent diffusion. The turbophoretic drift velocity is $-\tau_p\partial_z\overline{v_z'v_z'}$. The difference between (45) and the phenomenological diffusion equation (43) lies only in the diffusivity when v_d includes turbophoretic drift. The left panel in Fig. 8 shows the local fluid diffusivity $\epsilon_f = \sigma_u^2(z)\tau(z)$ (dotted line) and the particle diffusivity $\epsilon_{zz} = \tau_p(2E_z + \bar{\lambda}_{zz})$ (dash-dotted line) with $\bar{\lambda}_{zz}$ evaluated from the PT-data. The middle panel shows the drift velocity balance in (45) when using the non-local particle diffusivity ϵ_{zz}. Note that this balance is "exact" in the sense that it is consistent with the PT-results as shown above. The right panel shows the balance when the local fluid diffusivity ϵ_f is applied, keeping all other quantities unchanged (altering only the diffusive flux). The thick line shows the corresponding residual or imbalance in the equation.

The difference between a local approximation of fluid diffusivity and the inherently non-local particle diffusivity may resolve the issue raised by Mito and Hanratty (2005), where a local fluid diffusivity was found to be insufficient. These authors adjusted the diffusivity so as to minimize the residual in the mass flux balance. Their adjusted diffusivity (as displayed in their Fig. 17 for the lower half of the domain) is reduced relative to the fluid diffusivity, similar to the curve in Fig. 8 (left panel).

5. Discussion and conclusions

This work evaluates the applicability of approximate closure relations (dispersion tensors) in the kinetic theory of Reeks (1992) for particles suspended in inhomogeneous turbulence. The reference dispersion tensor components $\bar{\lambda}_{zz}$ and $\bar{\mu}_{zz}$ are evaluated using particle tracking (PT) based on a Langevin model for turbulence (e.g., Thomson, 1984 or Iliopoulos and Hanratty, 1999). Fully developed turbulent flow between two horizontal walls is considered. The concentration and particle kinetic stress (normal stress) obtained from the continuum equations is in agreement with the PT-data when the reference dispersion tensors are used.

For particles with small inertia, $\tau/\tau_p \gg 1$ (such that the particle relaxation time τ_p is typically smaller than the local correlation time τ of the fluid turbulence as seen by the particles), the locally homogeneous approximation (LHA) for the dispersion tensor $\bar{\lambda}_{zz}$ does not necessarily hold. This result is in contrast to the common view that the LHA-form is valid for low Stokes numbers when the relaxation time is small. In particular, the profile of $\bar{\lambda}_{zz}$ as function of z is skewed upwards (against gravity), while the LHA version is symmetric due to the underlying turbulence intensity profile. The value of $\bar{\lambda}_{zz}$ depends on the two-point correlation between the

fluid velocity at the evaluation point z and the fluid velocity sampled by the particle before it intersects the evaluation point. If the characteristic correlation time τ_{char} is significant (considering all particle paths in the ensemble), then $\bar{\lambda}_{zz}$ is sensitive to the non-local turbulence statistics, and it will deviate from the LHA value. In contrast, $\bar{\mu}_{zz}$ is close to the LHA value, since the relevant timescale is now the smaller relaxation time $\tau_{\text{p}} < \tau_{\text{char}}$ which enters into the velocity displacement Greens function. Only turbulence statistics in the immediate neighborhood of the evaluation point can then contribute to $\bar{\mu}_{zz}$.

By requiring constant density in the limit of passive tracer particles ($\tau_{\text{p}} \to 0$), it was shown that the body force due to the dispersion coefficient $\bar{\gamma}_z$ is related to $\bar{\lambda}_{zz}$ by $\bar{\gamma}_z = -\partial_z \bar{\lambda}_{zz}$. This defines a ''passive scalar approximation'' (PSA) which may be used as an approximation for $\bar{\gamma}_z$ in the current regime $\tau/\tau_{\text{p}} \gg 1$. The concentration profile obtained using this approximation is in excellent agreement with the PT data. In the intermediate regime, $\tau/\tau_{\text{p}} \sim 1$ one should expect that the PSA no longer holds, so that the general form of the momentum equation should be kept to account for the imbalance between $\bar{\gamma}_z$ and $\partial_z \bar{\lambda}_{zz}$. In this case, $\bar{\gamma}_z$ should be evaluated independently from $\bar{\lambda}_{zz}$.

By considering the diffusion form of the momentum equation, it is demonstrated that the particle diffusivity $\epsilon_{zz} = \tau_{\text{p}}(2E_z + \bar{\lambda}_{zz})$ should be applied and not the local fluid diffusivity. This supports the result of Mito and Hanratty (2005), where the effective diffusivity ϵ^* applied in the standard phenomenological diffusion equation $v_{\text{d}}\rho - \epsilon^* \partial_z \rho = 0$ to match the PT-data, does not correspond to the local fluid diffusivity. Even in the passive tracer limit (of zero relaxation time) the fluid diffusivity $\tau_{\text{p}} \bar{\lambda}_{zz}$ is not necessarily equal to a *local* approximation of the fluid diffusivity (say, represented by eddy viscosity).

Section 2.3 describes how the kinetic continuum equations can be solved for a fully developed channel flow. The fluid normal stress and the timescale τ is provided as input to these equations, while the normal kinetic stress of the particles, the particle diffusivity and the particle density profile are output quantities. For the current case of light particles ($\tau_{\text{p}}/\tau \ll 1$), the dispersion tensor component $\bar{\lambda}_{zz}$ can be evaluated a priori using particle tracking simulations, while $\bar{\mu}_{zz}$ and $\bar{\gamma}_z$ can be evaluated using the LHA-approximation and the PSA-approximation, respectively. An upcoming paper will discuss the properties of the theory for different particle inertia in the same channel flow configuration.

Acknowledgements

I thank M.W. Reeks, D.C. Swailes, Y.A. Sergeev and P. van Dijk of the University of Newcastle, UK, for valuable discussions and hospitality. This work has been funded by the Research Council of Norway via ''Strategic Institute Project ES132014, Droplet Transport Modeling and Generation Enhancement in Hydrocarbon Multiphase transport''.

References

Altunbaş, A., Kelbaliyev, G., Ceylan, K., 2002. Eddy diffusivity of particles in turbulent flow in rough channels. J. Aerosol Sci. 33, 1075.

Biberg, D., 2005. Mathematical Models for Two-phase Stratified Pipe Flow. PhD Thesis, University of Oslo.

Csanady, G.T., 1963. Turbulent diffusion of heavy particles in the atmosphere. J. Atmos. Sci. 20, 201.

Devenish, B.J., Swailes, D.C., Sergeev, Y.A., Kurdyumov, V.N., 1999. A PDF model for dispersed particles with inelastic particle-wall collisions. Phys. Fluids 11, 1858.

Hyland, K.E., McKee, S., Reeks, M.W., 1999. Derivation of a pdf kinetic equation for the transport of particles in turbulent flows. J. Phys. A: Math. Gen. 32, 6169.

Iliopoulos, I., Hanratty, T.J., 1999. Turbulent dispersion in a non-homogeneous field. J. Fluid Mech. 392, 45.

Kraichnan, R.H., 1970. Diffusion by a random velocity field. Phys. Fluids 13, 22.

Mito, Y., Hanratty, T.J., 2002. Use of a modified Langevin equation to describe turbulent dispersion of fluid particles in a channel flow. Flow Turbul. Combust. 68, 1.

Mito, Y., Hanratty, T.J., 2005. A stochastic description of wall sources in a turbulent field. Part 3: Effect of gravitational settling on the concentration profiles. Int. J. Multiphase Flow 31, 155.

Reeks, M.W., 1977. On the dispersion of small particles suspended in an isotropic turbulent fluid. J. Fluid Mech. 83, 529.

Reeks, M.W., 1992. On the continuum equations for dispersed particles in nonuniform flows. Phys. Fluids A 4, 1290.

Reeks, M.W., 1993. On the constitutive relations for dispersed particles in nonuniform flows. 1: Dispersion in a simple shear flow. Phys. Fluids A 5, 750.

Reeks, M.W., 2001. Particle drift in turbulent flows: the influence from local structure and inhomogeneity, ICMF 2001, New Orleans, 2001, No. 187.

Reeks, M.W., 2005a. On model equations for particle dispersion in inhomogeneous turbulence. Int. J. Multiphase Flow 31, 93.
Reeks, M.W., 2005b. On probability density function equations for particle dispersion in a uniform shear flow. J. Fluid Mech. 522, 263.
Sergeev, Y.A., Johnson, R.S., Swailes, D.C., 2002. Dilute suspension of high inertia particles in the turbulent flow near the wall. Phys. Fluids 14, 1042.
Swailes, D.C., Darbyshire, K.F.F., 1999. Probabilistic models for particle and scalar transport in fluctuating flows: an evaluation of simple closure approximations. Physica A 262, 307.
Swailes, D.C., Reeks, M.W., 1994. Particle deposition from a turbulent flow. 1. A steady state model for high inertia particles. Phys. Fluids 6, 3392.
Swailes, D.C., Sergeev, Y.A., Parker, A., 1998. Chapman–Enskog closure approximation in the kinetic theory of dilute turbulent gas-particulate suspensions. Physica A 254, 517.
Taylor, G.I., 1921. Diffusion by continuous movements. Proc. London Math. Soc. 151, 196.
Thomson, D.J., 1984. Random walk modeling of diffusion in inhomogeneous turbulence. Quart. J. R. Met. Soc. 110, 1107.
Zaichik, L.I., Alipchenkov, V.M., 2005. Statistical models for predicting particle dispersion and preferential concentration in turbulent flows. Int. J. Heat Fluid Flow 26, 416.